

NOTES AND CORRESPONDENCE

Anomalous Spiking in Spectra of XCTD Temperature Profiles

SARAH T. GILLE, AARON LOMBROZO, JANET SPRINTALL, AND GORDON STEPHENSON

Scripps Institution of Oceanography, La Jolla, California

RICHARD SCARLET

Lockheed Martin Sippican Sea-Air Systems, Marion, Massachusetts

(Manuscript received 25 August 2008, in final form 12 December 2008)

ABSTRACT

The high vertical resolution of temperature and salinity measurements from expendable conductivity–temperature–depth (XCTD) instruments can be useful for inferring small-scale mixing rates in the ocean. However, XCTD temperature profiles show distinct spectral spikes at frequencies of 5 and 10 Hz, corresponding to 1 and 2 cycles per five measurement points. Peaks at these same frequencies are often present in the conductivity spectra as well. The spectral spikes occur in XCTD profiles from both the subtropical and subpolar regions. They appear to originate as digital electronic noise within the probes. A finite impulse response filter design procedure was used to develop filters that could remove the spectral spikes while retaining as much high vertical resolution as possible. For most purposes, the application of an 11-point, least squares, low-pass filter proves sufficient for removing the spectral energy at 5 and 10 Hz, and results in an effective minimum vertical resolution of about 0.7 m.

1. Introduction

Expendable conductivity–temperature–depth probes (XCTDs) have recently been proven to provide a relatively inexpensive method for inferring the magnitude and spatial variability of small-scale mixing using the Thorpe scale technique (Thompson et al. 2007). XCTDs are relatively easy to deploy from a moving vessel even in rough sea-state conditions. This enables the collection of temperature and salinity measurements at higher sampling resolution in remote regions where the deployment of standard CTD instrumentation is often too risky or the required ship time is prohibitively expensive. Unlike CTDs, XCTDs cannot be recalibrated after deployment and there are lingering uncertainties about their fall rates, making the observations less accurate than traditional CTDs. Nonetheless, they have the potential to yield high

vertical resolution and are not subject to the problems of ship roll and self-induced turbulence that affect CTDs. These characteristics make XCTDs viable tools for investigating finescale mixing processes in the upper ~1000 m of the ocean.

One of the challenges in using XCTDs is determining the effective vertical resolution of the data. Figure 1 shows examples of XCTD upper-ocean profiles from the North Pacific (15.5°N, 139°E, 14 March 2001) and Drake Passage (57.03°S, 62.55°W, 5 July 2006). In the North Pacific, temperature and conductivity are highly stratified (Figs. 1a,b), whereas in the Drake Passage, temperature and conductivity have low stratification (Figs. 1c,d). In both regions, an expanded view of the point-to-point measurements shows an oscillation in a sawtooth pattern (see inset panels in Fig. 1). For example, Fig. 1 shows temperature alternating between 3.53° and 3.54°C twelve times over a distance of 2 m. Spectra computed from the temperature profiles show that this high-frequency noise is not simply random white noise, but results in two distinct spectral peaks at 5 and 10 Hz, corresponding to 1 and 2 cycles per five measurement points (Fig. 2a). Smaller spikes are present

Corresponding author address: Sarah Gille, Scripps Institution of Oceanography, 9500 Gilman Dr., Mail Code 0230, La Jolla, CA 92093–0230.
E-mail: sgille@ucsd.edu

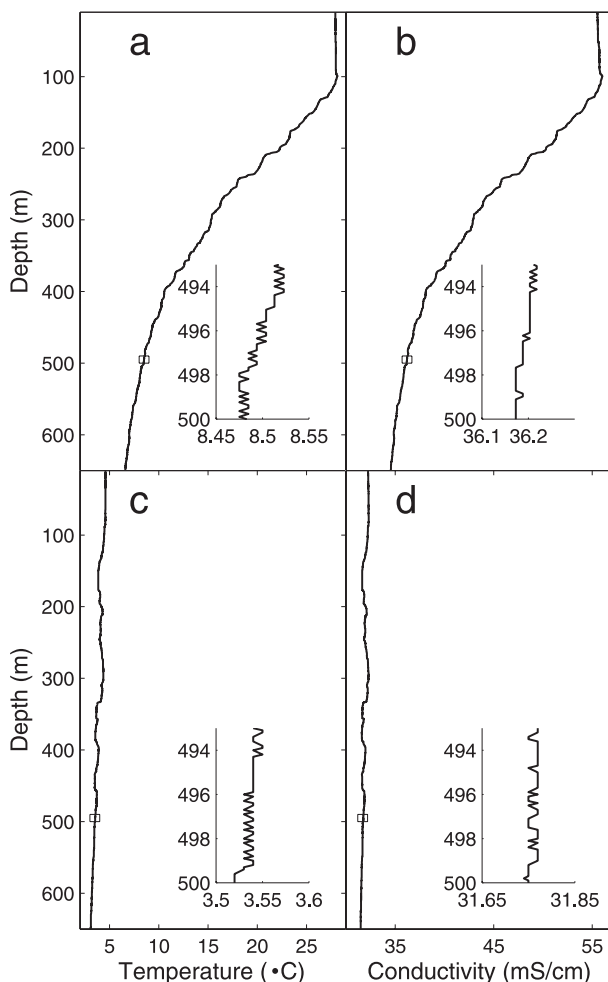


FIG. 1. XCTD profile of (a) temperature and (b) conductivity from the North Pacific Ocean (15.5°N, 139°E, 14 Mar 2001), and (c) temperature and (d) conductivity from Drake Passage (57.03°S, 62.55°W, 5 Jul 2006). The insets show expanded views from 493 to 500 m, highlighting the small-scale instrument noise. XCTDs sample at 25 Hz, providing roughly one sample every 13 cm.

in the conductivity spectra at the same frequencies (Fig. 2b). Energy associated with these noise peaks could contaminate analyses of lower-frequency processes if the profiles are not adequately filtered.

The objective of this study is first, to characterize the noise in XCTD temperature and conductivity observations and second, to evaluate appropriate strategies for filtering the noise while retaining the high-vertical wavenumber information. Section 2 discusses the XCTD instrumentation and XCTD measurements used in this study. Section 3 explores the causes of the spectral spikes, and section 4 evaluates low-pass filters to remove the spectral spikes without losing the high vertical structure. Results are summarized in section 5.

2. Data

a. The TSK XCTD system

Prior to 1999, XCTDs were manufactured by both Tsurumi Seiko Company, Ltd. (TSK) in Japan and Sippican Inc. (now a division of Lockheed Martin) in the United States. Based on a field test comparison in 1999, an arrangement between the two companies to supply only TSK digital XCTD probes to the global scientific community was established. The primary XCTD probes evaluated in this study are manufactured by TSK.

The conductivity and temperature sensors are installed at almost parallel positions in the nose of the probe, which has a central hole to allow the throughflow of seawater as the probe falls. Time constants of both sensors are nearly the same (100 ms or less) so as to minimize salinity spiking. Each XCTD is individually calibrated with three-point temperature and conductivity measurements that are stored internally within the probe. The thermistor resistance and conductivity cell output are transmitted back to the ship via conducting copper wire at a rate of 25 Hz.¹ The copper wire is dual spooled within the probe, and it is this mechanism that effectively decouples the XCTD probe from the impact of ship roll that can render CTD measurements ineffective for small-scale mixing studies. TSK XCTDs have an onboard microprocessor that converts raw measurements to the digitized signal that is transmitted up the wire to the ship (Hannon 2000). Signals are received using the Sippican MK-21 or the TSK MK-100 Data Acquisition System. Physical units of temperature and conductivity are then obtained using the three-point internally memorized calibration coefficients from the probe. The manufacturer's specification for the probe is 0.01°C resolution and 0.02°C accuracy for temperature, and 0.017 mS cm⁻¹ resolution and 0.03 mS cm⁻¹ accuracy for conductivity. This results in a specified accuracy of ~0.05 psu for salinity. The digitized data do not vary continuously but typically change values with increments of 0.01°C and 0.015 mS cm⁻¹.

TSK makes several models of XCTDs, which are rated to different depths and ship speeds for deployment. In this study we evaluate TSK XCTD-1 probes, which are rated to 1000 m at ship speeds of 12 kt. The fall rate

$$z = At - Bt^2$$

determines the depth (z) based on elapsed time (t) from when the probe hits the water surface. Several studies

¹ We do not consider XBTs in this study, since current models sample at 10 Hz, implying a lower vertical resolution.

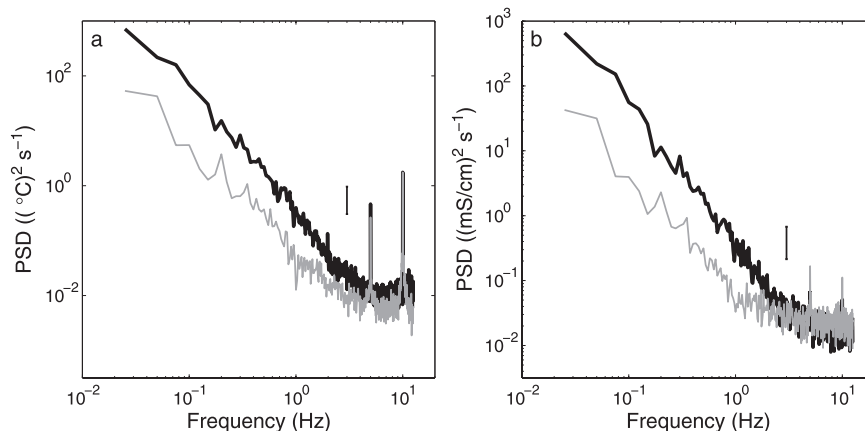


FIG. 2. Sample power spectral density of (a) temperature and (b) conductivity from XCTD profiles in the Pacific (black) and Drake Passage (gray). Spectra were calculated using detrended 1000-point records centered around 600-m depth for each of 12 profiles, then averaged together. Data from the North Pacific were collected from 1 to 13 Mar 2001. Data from Drake Passage were collected from 5 to 7 Jul 2006. The error bar is shown as a black vertical line. In the temperature spectra, the spikes at 5 and 10 Hz are significant in both ocean regions. In the conductivity spectra, the spikes are significant in Drake Passage but not in the North Pacific.

have examined the accuracy and choice of the XCTD fall-rate coefficients A and B through comparison with collocated CTD profiles (Johnson 1995; Alberola et al. 1996; Mizuno and Watanabe 1998; Kizu et al. 2008). Following the manufacturer's recommendation, in the fall-rate equation we use the coefficients of Mizuno and Watanabe (1998). The fall-rate parameters result in a vertical resolution for the XCTD profile of 13–14 cm. As with other free-falling expendable probes, depth is the greatest source of uncertainty (Wijffels et al. 2008), although a recent evaluation of XCTD measurements by Kizu et al. (2008) confirmed that the manufacturer's fall-rate coefficients are consistent with the reported accuracy of 2% (± 5 m) of depth, for depths greater than 20 m.

b. Field measurements

Most of the XCTD data used in this study were collected as part of the high-resolution (HR) XBT/XCTD transects. The HR program uses volunteer observing ships to maintain regularly repeated measurements of the upper-ocean properties using these expendable probes for studying the mean and variable mass and heat transport. In this analysis, we use the long time series available from near-exact repeat-location XCTD deployments from two HR transects chosen to represent different climatic regions (Fig. 3): World Ocean Circulation Experiment (WOCE) designated line PX-37 across the subtropical regime of the North Pacific Ocean, and line AX-22 across the Drake Passage. Occasionally an XCTD fails almost immediately after launch; here XCTD casts were considered only if they returned at

least 1000 data points, corresponding to a depth of about 150 m.

The zonal PX-37 spans from San Francisco, California, to Hong Kong, China (left panel of Fig. 3), generally via Honolulu, Hawaii, and Guam, and is typically undertaken every 3–4 months. XCTD sampling has been a part of this line since 1994. Along the transect, XCTDs are released at approximately 17 locations on each cruise. XCTD sampling is denser in the eastern boundary current regime of the California Current and transition region, where the frequent presence of eddies perturbs the water column (Sprintall and Roemmich 1999), and hence salinity variability becomes important for correctly estimating the geostrophic currents and transport (Gilson et al. 1998). For this study, a total of 145 XCTD profiles from PX-37 were used, all from TSK XCTD-1 probes with a TSK MK-100 data acquisition system and all collected since 2000.

Along the meridional AX-22 line across Drake Passage (right panel of Fig. 3), XBT/XCTD transects are undertaken 6–7 times per year, in all seasons, from the R/V *Laurence M. Gould*, the resupply vessel for the U.S. Antarctic Program. The ship follows one of three main tracks between Tierra del Fuego and various destinations along the Antarctic Peninsula (Sprintall 2003). While the XCTDs are released at approximately the same latitude on each of these tracks, the longitude is not always exactly repeated. Thompson et al. (2007) suggested that no significant variation in temperature and salinity profiles exists with longitude, and instead it is the variability associated with excursions of the Antarctic Polar Front (APF) that impacts the properties

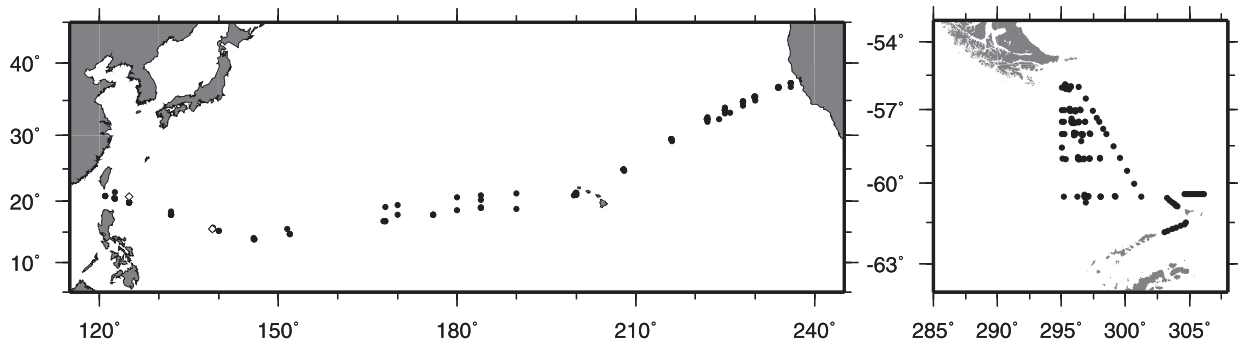


FIG. 3. Locations of XCTD casts used for this study. (left) WOCE XBT/XCTD transects PX-37 (trans-Pacific) and (right) WOCE XBT/XCTD transects AX-22 (circles) and southern Drake Passage (black diamonds). Spectral spiking was observed in all but two casts (identified by open diamonds).

within the Drake Passage. Beginning in December 2001, six XCTD profiles were obtained during each XBT transect across the 700-km-wide passage, and that was increased to twelve XCTDs in 2004 with higher sampling within the APF zone. A total of 138 XCTD profiles from AX-22 were used in this study, roughly evenly divided between summer and winter months. The TSK XCTD-1 probes were used with a MK-21 Sippican data acquisition system.

We also examined 24 XCTD profiles collected in July 2006 in the region of the Antarctic Peninsula from the R/V *Palmer* as part of a National Science Foundation (NSF) Office of Polar Programs–funded investigation of biology, iron distributions, and ocean circulation in the southern Drake Passage and Scotia Sea. The study released 24 XCTD-1 probes (right panel of Fig. 3, diamonds south of 60°S and east of 303°E) to provide more complete data in high-sea state, winter weather conditions.

3. Understanding the spike

In this section, we investigate the small-scale fluctuating pattern in the XCTD temperature and conductivity profiles (Fig. 1) with a goal of understanding the cause of this spectral spike. In the XCTD profiles of temperature with depth, a pattern of alternating values emerges when temperature is near the midpoint of two adjacent reportable values, with a slight syncopation from regular alternation (Fig. 1). This finescale fluctuation pattern is manifested in the spectra of the temperature profile as very energetic, narrow-band peaks at 5 and 10 Hz. Figure 2a shows sample temperature spectra for a 1000-point range centered around 600-m depth for the Drake Passage (black) and for the trans-Pacific transect (gray), both with statistically significant peaks at 5 and 10 Hz. A similar treatment of conduc-

tivity data (Fig. 2b) shows small peaks at 5 and 10 Hz in the trans-Pacific line, and statistically significant peaks in Drake Passage.

All of the available XCTD temperature profiles along HR lines AX-22 and PX-37 and from the south Scotia Sea project were examined for spectral peaks. Spectra were first whitened by multiplying by the wavenumber, and spikes were identified if a local maximum in the temperature spectrum occurred at either 5 or 10 Hz. Spectral spikes are easier to detect in low-stratification conditions. However, provided that data were detrended, spikes at 5 and/or 10 Hz were identifiable somewhere in the water column in all but two of the 307 XCTD temperature profiles that we examined (filled circles, Fig. 3), and in many cases we were able to detect spikes in all 1000-point records from the surface to the bottom of the casts. This was true regardless of acquisition system (MK-21 or MK-100), type of ship (ice breaker or container ship), latitude (subtropics or Southern Ocean), or season. The two Pacific profiles without spikes are indicated with open diamonds in the left panel of Fig. 3. These temperature profiles were in most respects like others from the western tropical Pacific, and their lack of apparent spectral spikes appears to be chance. (One additional shallow profile from the Drake Passage was not included in our analysis or plotted in Fig. 3, because the cast showed no evidence for spiking but was too shallow to evaluate whether spiking might occur deeper in the water column.) No spikes were identified in data from older model XCTDs, which used analog rather than digital electronics, and which also report data with coarser vertical resolution and therefore could not resolve the 5- and 10-Hz spectral peaks.

Conductivity profiles also consistently indicate spikes, though the spikes do not appear as large or as easy to detect as temperature spikes. Roughly 40% of Drake Passage profiles and about 20% of North Pacific profiles

show some evidence for conductivity spikes at 5 or 10 Hz. The difference between conductivity and temperature is likely because conductivity is inherently a noisier measurement. In Fig. 2, both temperature and conductivity spectra shift from being red at low frequencies to white at high frequencies, corresponding to a likely transition from low-frequency resolved signal to high-frequency noise. This transition occurs around 5 Hz for temperature but at lower frequency for conductivity, around 1 Hz for the low-stratification Drake Passage measurements (gray line in Fig. 2b).

The narrowness and high frequency of the spectral peaks and the ubiquity of their appearance in nearly all TSK XCTD casts regardless of location or season eliminates oceanographic processes as a likely cause. A number of characteristics of the finescale fluctuations in the measurements point to an electronic noise source associated with the digitization process. The magnitudes of the fluctuations correspond to the discretized resolution of the reported data, 0.01°C for temperature and 0.015 mS cm^{-1} for conductivity (Fig. 1). The spectral peaks are also visible in the raw data transmitted by the probe, so they appear to originate within the probe rather than in the deck unit software. The narrowband noise appears likely to originate from digital noise cross-over into analog electronics. The actual electronic noise could occur at a frequency higher than 10 Hz and be aliased to the 5- and 10-Hz peaks where we detect it.

Thus, the observed fluctuations in XCTD temperature and conductivity that result in the spectral peaks are inherent characteristics of the XCTD probes. They are within the noise specifications of the probes and should not be viewed as instrumental failures. Instrumental modifications to eliminate these spectral peaks might significantly increase the costs of the XCTDs, which are intended to be low-cost instruments. Since the spectral peaks are well defined and narrow, they can be suppressed by applying low-pass filters tuned to remove energy at frequencies greater than 5 Hz.

4. Optimal filter design

For certain applications of XCTD data, such as assessing Thorpe scales, we would like to retain as much high-resolution vertical structure as possible. Thompson et al. (2007) applied a triangle filter to their XCTD data, but did not extensively explore other filter options. In this section we consider whether the data can be optimally filtered to remove the spectral spikes without losing vertical structure.

We used a least squares finite impulse response (FIR) filter design procedure (Parks and Burrus 1987) to develop filters targeted specifically at the observed spec-

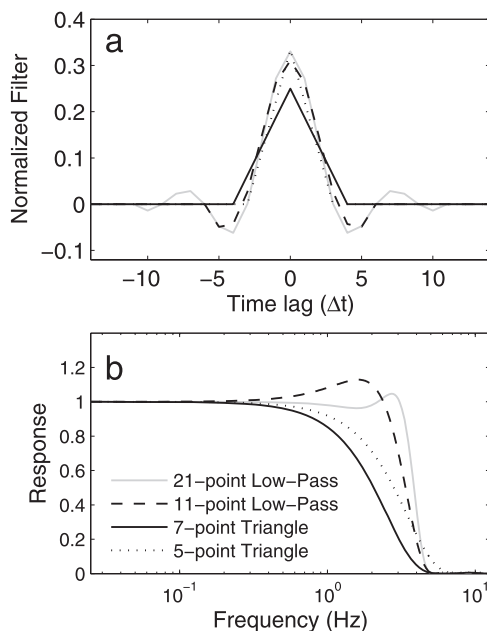


FIG. 4. Normalized (a) filter amplitude and (b) frequency response of 21-point low-pass (gray), 11-point low-pass (dashed), 7-point triangle (black), and 5-point triangle (dotted) filters. All filters are designed to remove energy at frequencies greater than 5 Hz.

tral spikes at 5 and 10 Hz (1 and 2 cycles per five observations), as described in the appendix. For both the North Pacific and the Drake Passage, temperature spectra are essentially white for frequencies greater than 5 Hz, implying that observations in these frequency ranges are likely to be dominated by noise. Even for conductivity measurements, which have white spectra at frequencies greater than 1 or 2 Hz, the largest sources of noise are the spikes at 5 and 10 Hz, so eliminating these spikes is likely to be critical. Thus we have focused on identifying an optimal low-pass filter to remove all energy at frequencies at or greater than the 5-Hz spike. The filtering process can distort data at the beginning or end of a record, so short filters are desirable, because they result in less data loss. However, long filters have the advantage of being easily tuned to remove a specific targeted frequency. We tested digital filters of lengths varying from 5 to 101 points. Ultimately we found that filters of 11 or 21 points could be tuned to remove high-frequency variability.

Figure 4a shows four filters that we examined in detail: 5- and 7-point triangle filters and 11- and 21-point low-pass filters computed using the least squares FIR. The 11- and 21-point filters have roughly the same structure as the 5-point triangle filter for short lags, while the 7-point triangle filter appears broader in the time domain. The appendix summarizes the parameters used to define the 11- and 21-point filters.

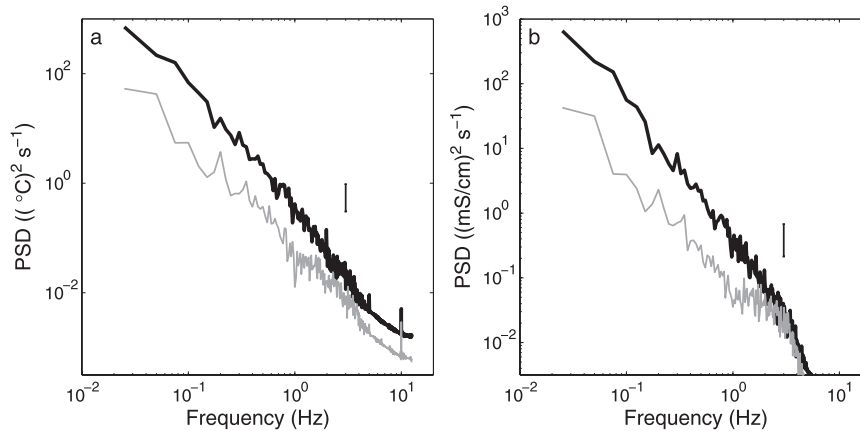


FIG. 5. Spectra of (a) temperature and (b) conductivity measurements as in Fig. 2 after application of an 11-point least squares low-pass filter.

The filter response shown in Fig. 4 indicates that all four filters remove most energy for frequencies of 5 Hz and greater, corresponding to an effective vertical resolution of 0.7 m. Because the 5-point triangle filter is narrow in the time domain, its response in the frequency domain is necessarily broad and decreases slowly to zero. Thus it has some residual energy at 5 Hz, meaning that data treated with the 5-point filter could contain residual noise associated with the 5-Hz spectral peak. The 7-point filter is more successful at removing the 5-Hz spectral peak but also attenuates energy at frequencies starting around 1 Hz. The 21-point filter is able to remove spectral energy associated with the 5- and 10-Hz noise peaks, without attenuating lower-frequency signals, but its broad width could result in more substantial data loss at the beginning and end of records.

For most purposes, the 11-point least squares FIR low-pass filter should do a good job of removing spectral energy that is likely to be due to noise, both at frequencies where the spectra are white and specifically at the 5- and 10-Hz noise peaks. Figure 5 shows temperature and conductivity spectra computed after applying the 11-point filter. For both the North Pacific and Drake Passage, the temperature spectra are red, with no significant energy at 5 or 10 Hz. The Drake Passage conductivity spectrum (gray line in Fig. 5b) shows some evidence for white noise between 1 and 5 Hz, suggesting that for some types of analysis in low-stratification regions, conductivity data should probably be low-pass filtered with a cutoff frequency around 1 Hz, corresponding to an effective vertical resolution of 3.5 m. In such a case, the exact spectral cutoff can be assessed from the available data, and an appropriate filter can be designed using the same FIR procedure used here.

Calculations of Thorpe scales are sensitive to spurious small inversions in potential density. Since XCTDs re-

port temperature only to an accuracy of 0.01°C and conductivity to 0.01 mS cm^{-3} , potential density is accurate to roughly 0.01 kg m^{-3} . At typical low-stratification regions found around 800-m depth in the Drake Passage, density changes of 0.01 kg m^{-3} occur over distances of 2.5–3.5 m, implying that the stratification should dictate the vertical resolution to be 2.5–3.5 m. Smaller-scale fluctuations that may be introduced when the data are filtered do not have physical meaning, and the data should therefore be truncated to the instrument precision before Thorpe scales are calculated. Figure 6 shows that truncating temperature and salinity can appear to add noise (relative to Fig. 5) within the frequency band above 5 Hz while decreasing energy and making the spectra redder between 1 and 5 Hz.

We use the truncated data, and following Thompson et al. (2007) compute Thorpe scales (L_T), dissipation rates (ϵ), and vertical diffusivities (κ). Estimates based on the 11-point filter described here exceed those obtained using the 21-point filter by less than 10% (and often by 1% or less), and results obtained using a 41-point filter with similar frequency cutoffs are also comparable in magnitude. These results are consistent within the statistical uncertainties of the calculation, though in general, higher-order filters can produce smaller values of L_T and κ . For comparison, in much of their analysis, Thompson et al. (2007) used a 99-point triangle filter, which removes energy above about 0.2 Hz, but they did not truncate the data to match the instrument accuracy. Low-pass filtering can either decrease or increase the estimates of L_T , ϵ , and κ . Modest levels of filtering merge small overturns to make them detectable, and decreasing the low-pass frequency cutoff progressively increases estimates of L_T , ϵ , and κ . However, very strong low-pass filters (such as the 99-point triangle) can suppress small overturns completely, and

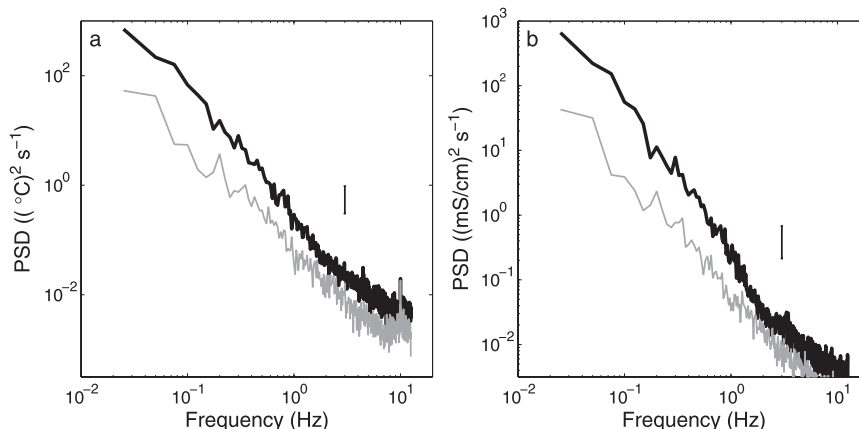


FIG. 6. Spectra of (a) temperature and (b) conductivity measurements as in Fig. 2 after application of the 11-point filter (as in Fig. 5) and truncation to match precision of digital data.

the result will be low values of L_T , ϵ , and κ . As an example, here, we find that at 57°S, relative to the 99-point triangle filter, estimates of ϵ and κ are 2.3 times larger when the 11- and 21-point filters are used, 2.9 times larger when the 5-point triangle filter is used, and 3 times larger when the 7-point triangle filter is used.

5. Summary

XCTD profiles of temperature and conductivity exhibit a distinct, slightly syncopated, sawtooth oscillatory pattern between discrete reported data values with increments of 0.01°C and 0.015 mS cm⁻¹. The fluctuations result in distinct, narrow, well-defined spectral peaks at 5 and 10 Hz, corresponding to 1 and 2 cycles per five measurement points. The spectral peaks are present in most XCTD profiles and are most obvious in regions of low background stratification. In all cases, the TSK XCTD temperature and conductivity sensors return data within the manufacturer's specified resolution.

The spectral peaks can be removed using a low-pass filter tuned to remove energy at frequencies greater than 5 Hz. Filtering at this scale corresponds to obtaining an effective vertical resolution of one wavelength per five measurements or about 0.7 m. An 11-point least squares FIR low-pass filter is suggested. Vertical resolution is also influenced by the numerical precision in the data. In low-stratification regions, vertical variations in salinity and correspondingly in potential density may not be resolved at small scales, and the effective vertical resolution may actually be closer to 3.5 m, corresponding to an effective 1-Hz sampling frequency.

As shown by Thompson et al. (2007), in studies of small-scale mixing, this resolution is sufficient for the detection of small-scale gravitationally unstable overturns in density profiles. The minimum thickness of a

resolvable overturn in the Thompson et al. (2007) study was reported to be 4 m, their smoothing scale for salinity. Although generally it is thought that the largest overturns contribute most to turbulent dissipation (Stansfield et al. 2001), in weakly stratified regions mixing may be underestimated if many small overturns are missed as the overturn detection becomes marginal. Implementing the 11-point filter recommended here would decrease the minimum detection thickness of an overturn more than threefold in regions with sufficient stratification, and perhaps improve the ability to resolve smaller overturns in low-stratification environments. Thus, while XCTDs do not have the accuracy obtainable by the microstructure measurements, they offer a readily deployable and cost-effective alternative in extreme environments for investigations of spatial variability in small-scale mixing rates.

Acknowledgments. Discussion with Andy Thompson and comments from the anonymous reviewers have helped clarify the ideas and presentation in this paper. This research was supported by grants from the National Science Foundation (OPP-0337998, OPP-0444134, OCE-0622740), from NOAA (NA17RJ1231 for the JIMO/SIO High Resolution XBT Network), and from NASA (JPL Contract 1224031).

APPENDIX

Defining the Low-Pass Filters

For this analysis, low-pass filters were computed using the Matlab implementation of a least squares, finite impulse response filter design procedure (Parks and Burrus 1987). We required that the filter retain no energy at frequencies equal to or greater than 1 cycle per

TABLE A1. Filter coefficients for 11- and 21-point low-pass filters. Note that filters are symmetric for positive and negative lags.

Time lag	21 point	11 point
0	0.3305	0.3105
1	0.2720	0.2627
2	0.1342	0.1471
3	0.0007	0.0269
4	-0.0619	-0.0430
5	-0.0474	-0.0491
6	-0.0004	
7	0.0286	
8	0.0228	
9	0.0001	
10	-0.0138	

five observations, or 40% of the Nyquist frequency. For the 11-point filter, we specified that for frequencies between 24% and 36% of the Nyquist frequency, spectral energy should taper from 1 to 0. For the 21-point filter, we specified a narrower tapering range, from 28% to 38% of the Nyquist frequency. These limits were adjusted through trial and error, and a more detailed investigation could more thoroughly consider alternate filter designs. Filter coefficients are summarized in Table A1.

REFERENCES

- Alberola, C., C. Millot, U. Send, C. Mertens, and J.-L. Fuda, 1996: Comparison of XCTD/CTD data. *Deep-Sea Res.*, **43**, 859–876.
- Gilson, J., D. Roemmich, B. Cornuelle, and L. L. Fu, 1998: The relationship of TOPEX/POSEIDON altimetric height to the steric height of the sea surface. *J. Geophys. Res.*, **103**, 27 947–27 965.
- Hannon, J., 2000: New developments in expendable oceanographic sensors and data acquisition systems. *OCEANS 2000 MTS/IEEE Conference and Exhibition Proceedings*, Vol. 3, MTS/IEEE, 1875–1877, doi:10.1109/OCEANS.2000.882210.
- Johnson, G., 1995: Revised XCTD fall-rate equation coefficients from CTD data. *J. Atmos. Oceanic Technol.*, **12**, 1367–1373.
- Kizu, S., H. Onishi, T. Suga, K. Hanawa, T. Watanabe, and H. Iwamiya, 2008: Evaluation of the fall rates of the present and developmental XCTDs. *Deep-Sea Res. I*, **55**, 571–586.
- Mizuno, K., and T. Watanabe, 1998: Preliminary results of in-situ XCTD/CTD comparison test. *J. Oceanogr.*, **54**, 373–380.
- Parks, T. W., and C. S. Burrus, 1987: *Digital Filter Design*. John Wiley and Sons, 342 pp.
- Sprintall, J., 2003: Seasonal to interannual upper ocean variability in the Drake Passage. *J. Mar. Res.*, **61**, 27–57.
- , and D. Roemmich, 1999: Characterizing the structure of the surface layer in the Pacific Ocean. *J. Geophys. Res.*, **104**, 23 297–23 311.
- Stansfield, K., C. Garrett, and R. Dewey, 2001: The probability distribution of the Thorpe displacement with overturns in Juan de Fuca Strait. *J. Phys. Oceanogr.*, **31**, 3421–3434.
- Thompson, A. F., S. T. Gille, J. A. MacKinnon, and J. Sprintall, 2007: Spatial and temporal patterns of small-scale mixing in Drake Passage. *J. Phys. Oceanogr.*, **37**, 572–592.
- Wijffels, S., J. Willis, C. Domingues, P. Barker, N. J. White, A. Gronell, K. Ridgeway, and J. A. Church, 2008: Changing expendable bathythermograph fall rates and their impact on estimates of thermocline sea level rise. *J. Climate*, **21**, 5657–5672.